Strong Cosserat elastic effects in a unidirectional composite

Zach Rueger and Roderic S. Lakes*

September 20, 2018

Department of Engineering Physics, Department of Materials Science
University of Wisconsin, Madison, WI 53706-1687, USA
Keywords (Cosserat, micropolar, generalized continuum)
* Corresponding author. email lakes@engr.wisc.edu Phone: +00 608 265 8697

Abstract

Strong Cosserat elastic effects are observed in a designed composite consisting of unidirectional corrugated tubes in a hexagonal array. The torsional characteristic length is much larger than the tube diameter. The effective coupling number N approaches its upper bound of 1. Extremely large size effects are observed, about a factor of 128 in torsion.

Preprint, Rueger, Z. and Lakes, R. S., Strong Cosserat elastic effects in a unidirectional composite, Zeitschrift fr angewandte Mathematik und Physik (ZAMP) 68:54, 9 pages, (2017).
DOI 10.1007/s00033-017-0796-6

1 Introduction

All physical materials have microstructure, but for many practical purposes it is useful to represent them as continuous media. Continuum theories with different degrees of freedom are available. An early theory of Navier [1], known as uniconstant elasticity, was based on a a theory assuming that forces act along the lines joining pairs of atoms and are proportional to changes in distance between them. It only allowed one elastic constant, a modulus. The theory was abandoned since it predicted a Poisson's ratio of 1/4 for all isotropic materials and experiments disclosed a range of Poisson's ratios. The currently accepted classical theory of elasticity has two independent isotropic elastic constants and allows for Poisson's ratios in isotropic materials to range from -1 to 1/2. Cosserat elasticity has more freedom than classical elasticity. The Cosserat theory [2], (with inertia terms called micropolar [3]) incorporates local rotations of points and a couple stress (a torque per unit area) as well as the translation and force stress (force per unit area) of classical elasticity; there are six independent isotropic elastic constants. A simpler variant presented by Koiter assumed that all the macrorotation and microrotation vectors are equal. This corresponds to $N = 1$, or equivalently κ approaching infinity in Cosserat elasticity. The Koiter [4] variant is called couple stress elasticity in which there are two characteristic lengths in addition to the classical constants: four isotropic elastic constants. The microstructure elasticity theory of Mindlin [5], also called micromorphic elasticity, has more freedom than classical or Cosserat elasticity; it allows points to translate, rotate, and deform within the media. This adds a high degree of complexity; for an isotropic solid, there are 18 micromorphic elastic constants compared with 6 for Cosserat elasticity and only 2 for classical elasticity.

The physical origin of the Cosserat couple stress is the summation of bending and twisting moments transmitted by the structural elements or ribs in materials. The local rotation in the Cosserat continuum corresponds to the rotation of the structural elements. Forces and moments are also considered in the classic analyses of foam by Gibson and Ashby [6] in which classical elastic moduli were determined; effects of rotation gradients were not considered.

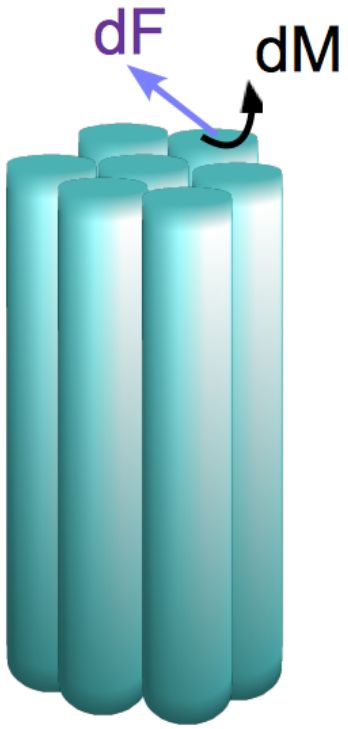

Figure 1: Composite containing unidirectional tubular inclusions with increment of force dF and increment of moment dM.

The constitutive equations for an anisotropic [3] Cosserat elastic solid are as follows.

$$\sigma_{ij} = C_{ijkl}\epsilon_{kl} + P_{ijkl}\phi_{k,l}, \tag{1}$$

$$m_{ij} = Q_{ijkl}\phi_{k,l} + P_{ijkl}\epsilon_{kl}, \tag{2}$$

in which C_{ijkl} is the elastic modulus tensor, ϵ_{kl} is strain, σ_{ij} is stress (symmetric in classical elasticity but asymmetric here), and the usual Einstein summation convention assumed in which repeated indices are summed over. m_{ij} is the couple stress tensor, moment per unit area, asymmetric in general. P_{ijkl} and Q_{ijkl} are Cosserat elastic constants that provide sensitivity to local (micro) rotation gradient. The Cosserat microrotation vector ϕ_i is kinematically distinct from the macrorotation vector $r_i = (e_{ijk}u_{k,j})/2$ associated with the motion of neighboring points.

The isotropic form [3] of the constitutive equations is as follows.

$$\sigma_{ij} = 2G\epsilon_{ij} + \lambda\epsilon_{kk}\delta_{ij} + \kappa e_{ijk}(r_k - \phi_k) \tag{3}$$

$$m_{ij} = \alpha\phi_{k,k}\delta_{ij} + \beta\phi_{i,j} + \gamma\phi_{j,i} \tag{4}$$

There are six independent isotropic Cosserat elastic constants λ, G, α, β, γ, κ. Physically, λ, a Lamé constant from elasticity theory, is an elastic modulus component which couples a strain in one direction with stress in a perpendicular direction with all other strains held constant. The physical meaning of G, shear modulus, is the resistance to shear deformation. α, β, and γ provide sensitivity to rotation gradients while κ is a modulus which quantifies the coupling between macro and micro rotation fields [29]. The following technical constants, beneficial for physical insight, are obtained from them. As in classical elasticity, several are interrelated; specifically of the seven below, the classical relation between E, G and ν applies.

$$Young's\ modulus \qquad E = \frac{G(3\lambda + 2G)}{\lambda + G} \tag{5}$$

$$Shear\ modulus \qquad G \tag{6}$$

$$Poisson's\ ratio \qquad \nu = \frac{\lambda}{2(\lambda + G)} \tag{7}$$

$$Characteristic\ length,\ torsion \qquad \ell_t = \sqrt{\frac{\beta + \gamma}{2G}} \tag{8}$$

$$Characteristic\ length,\ bending \qquad \ell_b = \sqrt{\frac{\gamma}{4G}} \tag{9}$$

$$Coupling\ number \qquad N = \sqrt{\frac{\kappa}{2G + \kappa}} \tag{10}$$

$$Polar\ ratio \qquad \Psi = \frac{\beta + \gamma}{\alpha + \beta + \gamma}. \tag{11}$$

Cosserat elasticity has the following consequences. A size effect is predicted in the torsion [7] and bending [8] of circular cylinders of Cosserat elastic materials. Slender cylinders appear to be stiffer than expected classically. A similar size effect is also predicted in the bending of plates. No size effect is predicted in tension or compression. The stress concentration factor for a circular hole is smaller than the classical value, and the small holes exhibit less stress concentration than larger ones [9]. However, classical elastic solids do not exhibit size effects in torsion or bending; structural rigidity goes as the fourth power of the radius. Also, in classical elasticity, stress concentration is independent of hole size.

Cosserat elastic effects have been observed experimentally. Size effects observed to occur in torsion and bending of closed cell foams [10, 11], open cell foam [12], negative Poisson's ratio foam [13], and compact bone [14] are consistent with Cosserat elasticity. The apparent modulus increases substantially as the specimen diameter becomes smaller, in contrast to the prediction of classical elasticity. Large material microstructure size does not guarantee Cosserat elasticity: a composite containing aluminum beads in an epoxy matrix was tested for such effects and found to behave according to classical elasticity [7]. Although Cosserat effects are not guaranteed in materials with large microstructure, the work presented here will demonstrate that these materials can not only demonstrate the aforementioned effects, but also show effects of large magnitude.

The Cosserat characteristic length was determined in a two dimensional polymer honeycomb [15]. Full field measurements of deformation reveal non-classical elastic effects that are consistent with Cosserat elasticity. Warp of a bar of rectangular cross section in torsion is predicted to be reduced in a Cosserat elastic solid [16]. The corresponding non-classical strain field was observed in a compact bone [17]. Deformation spills over into the corner region where it would be zero in classical elasticity [18] as revealed by holography. This improves strain concentration. Strain at the corner entails asymmetry of the stress as predicted by Cosserat elasticity. The reduction of warp

deformation has been observed via holography [19]. As for plastic deformation, rotational plastic deformation mechanisms were interpreted via gradients in a micropolar continuum theory [20].

The present research deals with experimental study of size effects and Cosserat elasticity in a designed composite consisting of unidirectional corrugated tubes and silicone rubber matrix in hexagonal arrays. Each tube is intended to carry a force and a moment as shown in Figure 1.

2 Methods

2.1 Materials and experiment

Corrugated nylon tubing, manufactured by Waytek [21], with inner diameter of 3.18 mm (0.125 in), outer diameter of 6.7 mm, and density of approximately 0.26 g/cm^3 was used. Lengths of tubing were cut with a hot wire cutter such that the length of the array of tubes was three times longer than the average diameter of the sample. The corrugated tubing came coiled and was straightened by running a brass tube with an outer diameter of approximately 3 mm through 20 cm lengths of the tubing and heating it in a convection oven at 105°C for two hours. After two hours the straightening apparatus was removed and allowed to cool for 15 minutes before removing the straightened section of corrugated tubing. Four samples were created and tested beginning with a single tube, followed by an array of three tubes arranged in a triangular formation, then seven tubes arranged in a hexagonal pattern, and finally 19 tubes again arranged in a hexagonal formation. The largest of these specimens is shown in Figure 2a as well as its hexagonal array cross-section, Figure 2b.Because the broadband viscoelastic spectrometer (BVS) used for testing could not accommodate larger specimens than the one in Figure 2a, the number of specimens was limited to four. A fifth datum was obtained for the asymptotic modulus in the absence of gradients. This was done by a compression test for axial deformation and by a composite analysis for shear deformation. The lengths of tubing were glued together with approximately 1 mm spacing between each tube using Loctite clear silicone sealant. The entire sample was allowed to cure for two days per product directions prior to testing. The resulting specimens had an average density of 0.46 ± 0.07g/cm^3. After curing, the ends of the samples were sanded flat using metallography sanding wheels. Circular end pieces larger than the diameter of the sample were cut from 0.6 mm thick aluminum plate and cemented to both bases of the sample using cyanoacrylate (Loctite 401) over the entire surface. Pressure was applied to the end pieces to ensure good adhesion. A catalyst was applied to the surfaces to reduce the amount of cement used and to improve the bond.

These specimens were tested for torsional and bending rigidity using a broadband viscoelastic spectrometer (BVS). This instrument makes use of a dual Helmholtz coil acting upon a magnet attached to the specimen to generate torque. The coil spacing is smaller than the larger specimens so a short alumina stalk with a magnet on the end was fixed to one of the aluminum end plates. Because the rigidity of the specimens was not sufficiently different from the rigidities of the alumina stalk or cement bond between stalk and end plate, a mirror was fixed to the edge of the face opposite of the alumina stalk on the same end plate. This placement eliminated any measured loss of motion from the magnet to the specimen. The magnet was calibrated using the BVS and a lock-in amplifier. The magnetic calibration constants of this particular magnet were obtained by testing a 6061 aluminum alloy rod of known elastic properties; the calibration constants were $8.18 * 10^{-6}$ Nm/A in torsion and $1.33 * 10^{-5}$ Nm/A in bending. The free end plate of specimens was cemented to a steel adapter which was screwed into a 25 mm thick steel rod for holding the specimen inside the BVS. Prior to testing, viscoelastic strain was allowed to recover overnight to enable stable measurements. The specimen was lowered into the BVS such that the magnet was centered in the Helmholtz coils of the BVS. The lower limit on specimen size was limited to the

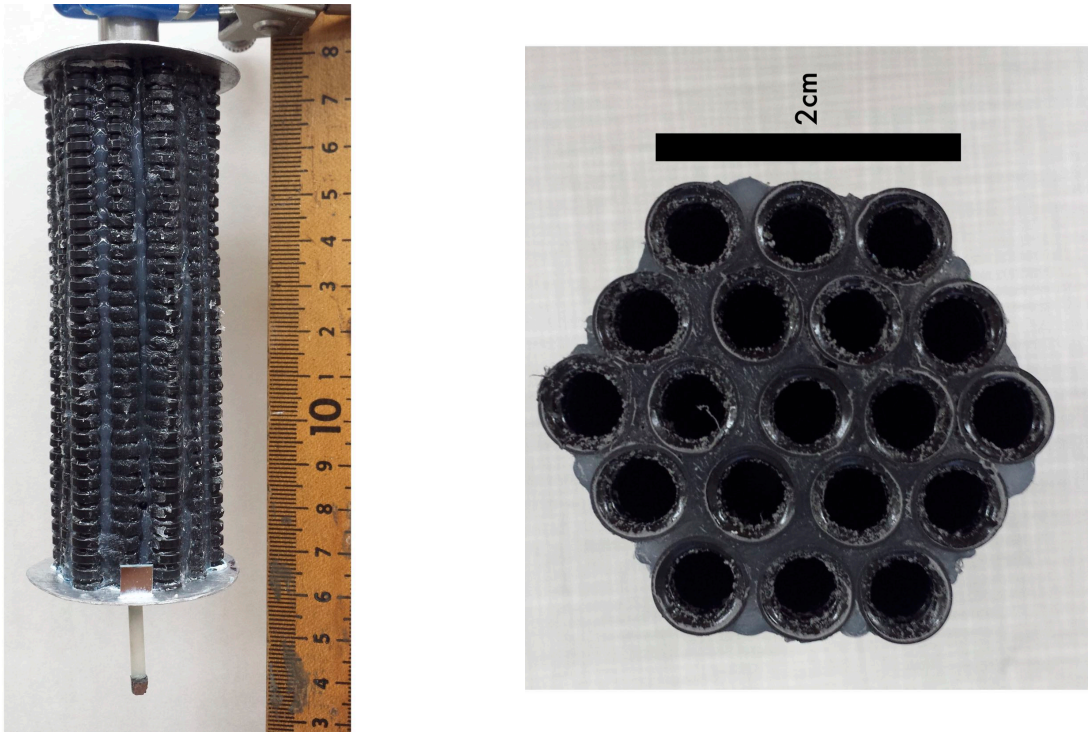

(a) (b)

Figure 2: (a) Largest specimen of aligned corrugated tubing and silicone rubber matrix composite. (b) Cross section of largest sample.

diameter of an individual corrugated tube.

Deformation was measured using the BVS via a semiconductor laser beam reflected from the mirror attached to the lower aluminum end plate onto a four quadrant silicon light detector. Prior to each test the silicon light detector was calibrated by aligning the laser beam so that its position could be measured. The light detector was moved a known amount in either the horizontal or vertical direction, for torsion and bending respectively, using a calibrated stage. The resulting measurement of output voltage per change in position, measured in μm, was used as the beam position calibration constant (V/μm).

To test the specimens a sinusoidal signal with a frequency of 1 Hz, well below any resonant frequencies, from a function generator (SRS Model DS345) was input to the torsion Helmholtz coil. Because the same frequency was used for all specimens, viscoelastic effects are decoupled from the size effects to be probed. The torque signal was obtained as the voltage across a 1Ω resistor in series with the coil to eliminate effects of inductive reactance from the coil. The torque signal vs. angular displacement signal was displayed on a digital oscilloscope (Tektronix TDS3014B) using DC coupling. The torque and angle signals were displayed as a Lissajous figure and used to calculate the modulus of the specimen. The maximum strain during testing was less than $1.1 * 10^{-7}$. This is will within the range of linearity for this material. For bending, the light detector mode was switched to vertical detection and the beam position calibration constant was adjusted accordingly; the driving signal was input to the orthogonal bending Helmholtz coil.

Compression tests were conducted to ascertain the behavior of the largest specimen in the absence of macroscopic gradients of strain and rotation. This was done using a servo-hydraulic load frame driven at a sinusoidal frequency of 1 Hz. The output stress and strain signals were

displayed on a digital oscilloscope as a Lissajous figure so that the modulus of the specimen could be calculated. Poisson's ratio was also determined using compression testing by measuring the transverse strain with a micrometer.

2.2 Analysis and interpretation

Size effect results were interpreted using available exact analytical solutions involving Bessel functions for torsion and bending of a Cosserat elastic solid andapproximating the cross-section of each specimen as circular. Isotropic solutions are used because no anisotropic solutions are available. Elastic constants obtained are technical constants. This is in the same vein as classical constants obtained from quasistatic tests rather than ultrasonic tests on anisotropic solids. Size effects manifest as higher effective moduli in slender specimens than thick ones. The classical torsional rigidity is $\frac{M}{\theta} = G[\frac{\pi}{2}r^4]$. For Cosserat elasticity in this regime, $\frac{M}{\theta} = G[\frac{\pi}{2}r^4](1 + 6(\ell_t/r)^2)$. G is the true shear modulus in the absence of gradients; M is applied moment and θ is angular displacement. This expression is exact for $N = 1$; for other N the exact solution involves Bessel functions [7]:

$$\Omega = (1 + 6(\ell_t/r)^2)[\frac{(1 - 4\Psi\chi/3)}{1 - \Psi\chi}], \tag{12}$$

in which $\chi = I_1(pr)/prI_0(pr)$, $p^2 = 2\kappa/(\alpha + \beta + \gamma)$ and I_0 and I_1 are modified Bessel functions of the first kind. The constant Ψ only has an appreciable influence for very small radius specimens.

Because of the limitations of testing large samples imposed by the size of the BVS an asymptote of torsional rigidity vs. diameter could not be determined directly from this method. The asymptotic value of G was calculated from durometer measurements upon a separate cured block of silicone and from the Reuss relation in which tubes and silicone rubber were considered as constituents. ℓ_t and the value N were determined by fitting the entire set of experimental data to Eq. 12 using MATLAB. In order to fit Eq. 12 to the data, the thermodynamic lower bound of zero was applied to ℓ_t, and an upper bound of 1 was set for N. To accelerate convergence, an upper limit of 100 mm was chosen for ℓ_t.

For bending, the classical bending rigidity is $\frac{M}{\theta} = E[\frac{\pi}{4}r^4]$. For bending of a Cosserat elastic circular rod and radius r, the rigidity ratio is approximately

$$\Omega \approx 1 + 8(\ell_b/r)^2\frac{(1 - (\beta/\gamma)^2)}{(1 + \nu)}. \tag{13}$$

The expression is approximate for small bending characteristic length $\ell_b << r$. The exact form, involving Bessel functions, is

$$\Omega = 1 + 8(\ell_b/r)^2\frac{(1 - (\beta/\gamma)^2)}{(1 + \nu)} + \frac{8N^2}{(1 + \nu)}[\frac{(\beta/\gamma + \nu)^2}{\zeta(\delta a) + 8N^2(1 - \nu)}] \tag{14}$$

with $\delta = N/\ell_b$ and $\zeta(\delta r) = (\delta r)^2[((\delta r)I_0((\delta r)) - I_1((\delta r)))/((\delta r)I_0(\delta r) - 2I_1(\delta r))]$.

Similarly for bending, the asymptotic value of E was impossible to determine via BVS experimentation because of size limitations. Consequently, compression testing was performed to determine the value. Longitudinal compression testing was conducted to calculate Poisson's ratio for bending calculations. The remaining parameters, N, β/γ, and ℓ_b, were determined by fitting the entire set of experimental data for bending to Eq. 14 using MATLAB. To allow fitment, the thermodynamic lower bound of zero was used for ℓ_b; similarly, the allowed range for N is from zero to one and β/γ from -1 to 1.

3 Results and discussion

Density of corrugated tubing specimens composed of more than one tube was independent of size to within ten percent. The single tube specimen was about half of the density of the larger specimens on average. The discrepancy in density was cause by the silicone rubber matrix in samples composed of more than one segment of tubing.

Results of torsion size effect studies are shown in Figure 3.

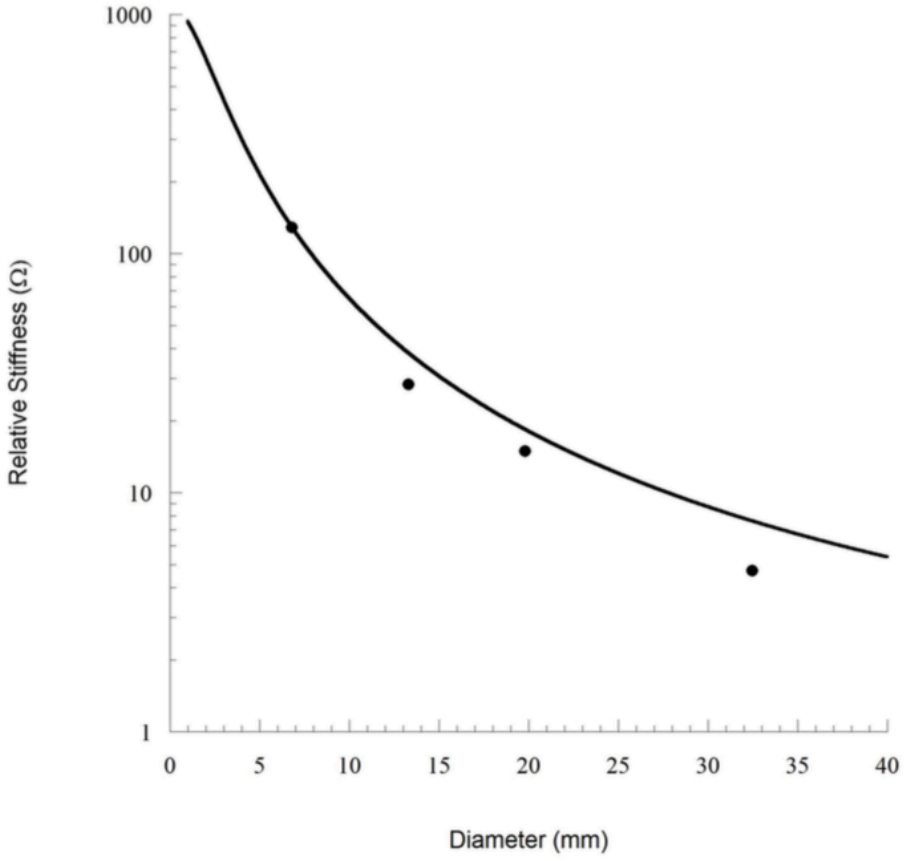

Figure 3: Size effects for corrugated tubing specimens in torsion. Points are experimental. Curve is theoretical for $G = 890$ kPa, $\ell_t = 17.3$ mm $N = 0.996$ and $\Psi = 1.5$. Classical elasticity ($\ell_t = 0$) predicts constant $\Omega = 1$ independent of diameter.

For corrugated tubing specimens in torsion, $G = 890$ kPa, $\ell_t = 17.3$ mm $N = 0.996$ and $\Psi = 1.5$ when Poisson's ratio is 0.3. The goodness of fit was $R^2 = 0.99$. The maximum size effect in torsion was $\Omega = 128.8$. The asymptotic value of G was located by using a durometer to determine the modulus of the silicone matrix materials used in the composite. The inferred Young's modulus of the silicone was approximately 1 MPa so the shear modulus is 0.33 MPa. By measuring the volume fraction of the silicone rubber matrix and using the Reuss relation, the asymptotic shear modulus for the composite was calculated to be 0.89 MPa.

Results of bending size effect studies are shown in Figure 4.

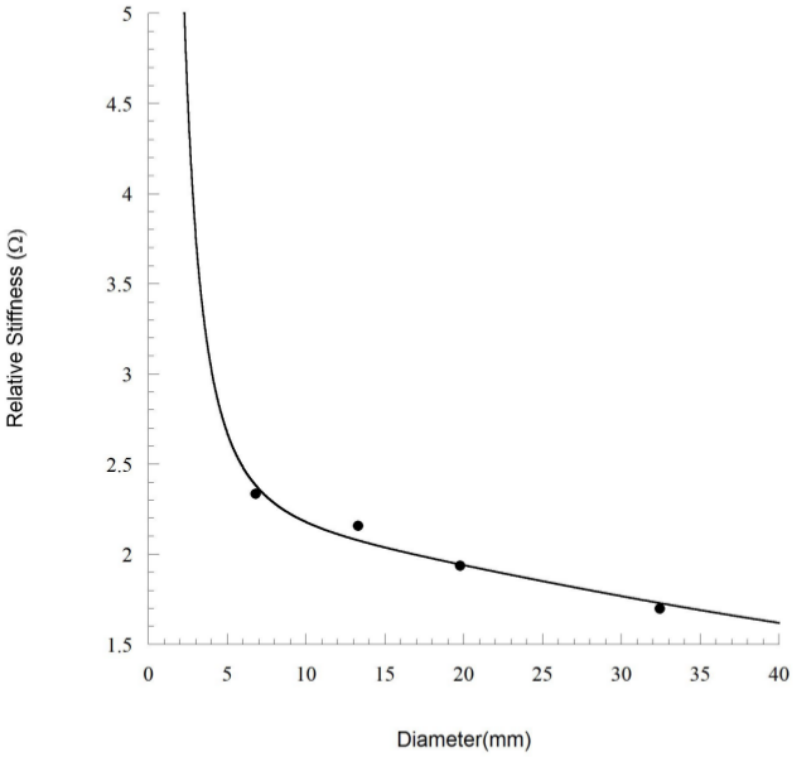

Figure 4: Size effects for corrugated tubing specimens in bending. Points are experimental. Curve is theoretical for $\beta/\gamma = 0.995$, $N = 0.999$, $E = 14.2$ MPa, and $\ell_b = 7.91$ mm. Classical elasticity predicts constant $\Omega = 1$ independent of diameter.

Initial fitting of the data using the asymptotic value for E found from compression testing at 1 Hz, 14.2 MPa, and the Poisson's ratio 0.0 ± 0.1 found from compression testing yielded poor results. This is attributed to the single measurement of Poisson's ratio from longitudinal compression testing and the anisotropic structure of the specimens. The isotropic analytical solution links Poisson's ratio to the size effects; this is not expected in anisotropic solids. When subsequent fits were performed using an asymptotic value for E of 14.2 MPa and allowing Poisson's ratio to vary in addition to the other fitting parameters and elastic constants, $\nu = 0.3$, $\ell_b = 7.91$ mm, $\beta/\gamma = 0.995$, and N = 0.999. The goodness of fit was $R^2 = 0.96$. The largest size effect in bending under these conditions was $\Omega = 2.33$. Because the composite specimens were anisotropic the characteristic length of bending was independent from the characteristic length of torsion. Also due to the anisotropy of the specimens, the coupling number, N, from torsion is not necessarily applicable to bending results which is why the N in this fit was allowed to varied. However, the N calculated from torsion experiments is very similar to the N calculated from bending experimentation.

The material has hexagonal structural symmetry, so it is elastically anisotropic. Consequently the properties obtained from the experiments are technical constants, not tensorial constants. This is analogous to materials testing in classical elasticity in which it is not always practical to incorporate a full anisotropic interpretation. The elastic symmetry of such a hexagonal structure is transversely isotropic which means properties in the transverse directions are independent of direc-

tion. That provides some simplification in the classical case; nevertheless no analytical solutions for Cosserat elasticity are known for such symmetry. Therefore the isotropic solutions are used and the elastic constants are interpreted as technical constants. Anisotropy cannot be a confounding variable because there are no size effects in classical elasticity even in the anisotropic case [23].

As for comparison with theory, no known analysis is available for the structure of the present material. Cosserat elastic constants have been calculated from theoretical homogenization of several lattices with straight ribs [24] [25] [26]. These are stretch dominated so the effects of rib bending and torsion are much smaller than the effects of rib extension. The characteristic lengths of such lattices are much smaller than the cell size. Two dimensional chiral honeycomb lattice structures analyzed as Cosserat continua disclosed bend dominated behavior in which Young's modulus is governed by rib bending. These honeycombs have large N approaching its upper bound 1, and characteristic length ℓ comparable to the cell size [27]. Sigmoid curvature of the lateral surfaces of bent square cross section bars was analyzed via Cosserat elasticity [28]. Such curvature requires $\beta/\gamma \neq -\nu$ and indeed it was observed in conventional as-received open cell foam. Although no formal measurements were made with the negative Poisson's ratio foam (for which $\beta/\gamma \approx -\nu$), visual observation of such bending of a square cross section bar suggested any sigmoid curvature must be small.

In summary, large size effects are observed in the torsion of aligned corrugated tubing and silicone rubber matrix composites. The effects are consistent with Cosserat elasticity. Results do not necessarily exclude the presence of additional freedom such as that incorporated in micromorphic / Mindlin microstructure [5] theory or in microstretch elasticity [22].

4 Conclusions

Large size effects are observed in the torsion and bending of aligned corrugated tubing and silicone rubber matrix composites. These effects are inconsistent with classical elasticity, but can be modeled with Cosserat elasticity. The torsional characteristic length is much larger than the tube diameter.

5 Acknowledgements

We gratefully acknowledge support of this research by the National Science Foundation via Grant CMMI-1361832.

References

[1] S. P. Timoshenko, History of Strength of Materials, Dover, NY, (1983).

[2] Cosserat, E. and Cosserat, F., 1909, *Theorie des Corps Deformables*, Hermann et Fils, Paris.

[3] A. C. Eringen, Theory of micropolar elasticity. In *Fracture*, 1, 621-729 (edited by H. Liebowitz), Academic Press, NY (1968).

[4] Koiter, W. T., 1964, Couple-Stresses in the theory of elasticity, Parts I and II, Proc. Koninklijke Ned. Akad. Wetenshappen **67**, pp. 17-44.

[5] Mindlin, R. D., Micro-structure in linear elasticity, Arch. Rational Mech. Analy, **16**, 51-78, (1964).

[6] L.J. Gibson and M.F. Ashby, Cellular Solids, 2nd ed., Pergamon, Cambridge, (1997).

[7] R. D. Gauthier and W. E. Jahsman, A quest for micropolar elastic constants. J. Applied Mechanics, **42**, 369-374 (1975).

[8] G. V. Krishna Reddy and N. K. Venkatasubramanian, On the flexural rigidity of a micropolar elastic circular cylinder, J. Applied Mechanics **45**, 429-431 (1978).

[9] R. D. Mindlin, Effect of couple stresses on stress concentrations, Experimental Mechanics, **3**, 1-7, (1963).

[10] R. S. Lakes, Experimental microelasticity of two porous solids, Int. J. Solids and Structures, **22**, 55-63 (1986).

[11] W. B. Anderson and R. S. Lakes, Size effects due to Cosserat elasticity and surface damage in closed-cell polymethacrylimide foam, J. Materials Science, **29**, 6413-6419 (1994).

[12] Z. Rueger and R. S. Lakes, Experimental Cosserat elasticity in open cell polymer foam, Philosophical Magazine, **96**, 93-111 (2016).

[13] Z. Rueger and R.S. Lakes, Cosserat elasticity of negative Poisson's ratio foam: experiment, Smart Materials and Structures, accepted 11.9 (2015).

[14] R. S. Lakes, On the torsional properties of single osteons, J. Biomechanics, **28**, 1409-1410 (1995).

[15] R. Mora and A. M. Waas, Measurement of the Cosserat constant of circular cell polycarbonate honeycomb, Philosophical Magazine A, **80**, 1699-1713 (2000).

[16] H. C. Park and R. S. Lakes, Torsion of a micropolar elastic prism of square cross section. Int. J. Solids, Structures, **23**, 485-503 (1987).

[17] H. C. Park and R. S. Lakes, Cosserat micromechanics of human bone: strain redistribution by a hydration-sensitive constituent, J. Biomechanics, **19**, 385-397 (1986).

[18] R. S. Lakes, D. Gorman, and W. Bonfield, Holographic screening method for microelastic solids, J. Materials Science, **20**, 2882-2888 (1985).

[19] W. B. Anderson, R. S. Lakes, and M. C. Smith, Holographic evaluation of warp in the torsion of a bar of cellular solid, Cellular Polymers, **14**, 1-13 (1995).

[20] R.D. Nyilas, M. Kobas and R. Spolenak, Synchrotron X-ray microdiffraction reveals rotational plastic deformation mechanisms in polycrystalline thin films, Acta Mater. **57** 3738-3753 (2009).

[21] Waytek, Incorporated, Chanhassen, MN.

[22] A. C. Eringen, Theory of thermo-microstretch elastic solids, Int. J. Engng. Sci., **28** (12) 1291-1301, (1990).

[23] Lekhnitskii, S. G., *Theory of elasticity of an anisotropic body*, Mir, Moscow, (1981).

[24] A. Askar and A. S Cakmak, A structural model of a micropolar continuum, Int. J. Engng. Sci. **6**, 583-589, (1968).

[25] T. Tauchert, A lattice theory for representation of thermoelastic composite materials, Recent Advances in Engineering Science, **5**, 325-345 (1970).

[26] G. Adomeit, Determination of elastic constants of a structured material, Mechanics of Generalized Continua, (Edited by Kröner, E.), IUTAM Symposium, Freudenstadt, Stuttgart. Springer, Berlin (1967).

[27] A. Spadoni and M. Ruzzene, Elasto-static micropolar behavior of a chiral auxetic lattice, J. Mechs Physics of Solids, **60**, 156-171 (2012).

[28] R. S. Lakes and Drugan, W. J., Bending of a Cosserat elastic bar of square cross section - theory and experiment, J. Applied Mechanics, **82**(9), 091002 (2015).

[29] R. S. Lakes, Physical meaning of elastic constants in Cosserat, void, and microstretch elasticity, Journal of Mechanics of Materials and Structures, **11**, 217-229 (2016).